Article

Spiral Structured Cellulose Acetate Membrane Fabricated by One-Step Electrospinning Technique with High Water Permeation Flux

Allison A. Kim [1],* and Milan Babu Poudel [2],*

1   Department of Healthcare Management, Woosong University, Daejeon 34606, Republic of Korea
2   Department of Convergence Technology Engineering, Jeonbuk National University,
    Jeonju 54896, Republic of Korea
*   Correspondence: allisonkim@wsu.ac.kr (A.A.K.); poudelmeelan@jbnu.ac.kr (M.B.P.)

Abstract: A functionally graded membrane (FGM) with a special spiral-structured cellulose acetate (CA) membrane was prepared by electrospinning under different collection distances. The membrane morphology was analyzed by scanning electron microscopy (SEM). FESEM images revealed that the high concentration shows the formation of fibers with an irregular diameter, with a large diameter distribution range. The fiber collected at a short distance of 10 cm experiences the strong electrostatic force, resulting in the short flight time for the polymer jet. This causes the bending instability of the polymer jet forming the comparatively thick fiber diameters, whereas the fiber collected at 15 cm shows the presence of a smooth, homogeneous diameter. Furthermore, the water flux of the membrane was determined using 50 mL of Amicon stirred cells. The fiber collected at different distances showed diameter variation, which is used to design a special spiral structure on the membrane by auto-moving the collector between the fixed distances of 10–20 cm. This technique will reveal a new approach for the fabrication of a special spiral structure on the nanofibrous membrane for different biomedical applications from different polymers. Meanwhile, the fabricated FGM with a special spiral-structure CA membrane demonstrates high water permeation flux.

Keywords: cellulose acetate membrane; electrospinning; FGM; spiral structure

1. Introduction

Electrospinning is broadly applied for nanofiber fabrication with unique and advanced properties [1,2]. It was first reported in 1914 by Zeleny [3], but the US patented it by Formhals in 1934 [4]. In this process, a high-voltage power supply was used between the spinneret and fiber collector to inject the polymer solution [5,6]. When the applied voltage reaches above a certain threshold value, the charged jet of the polymer solution is taken out from the spinneret tip and is accelerated toward the grounded collector [7–10]. During the flight of the charged jet in the air, the solvent molecules escape, and the long polymer thread entanglement leads to the formation of a fine nonwoven nanofiber on the collector [11,12]. The electrospinning can fabricate a highly porous nano-fibrous mesh with a high surface-to-volume ratio, which amends the performance in diverse fields [13–15]. The relatively high production rate and simplicity in establishment make electrospinning an attractive technique for industrial, as well as academic, research fields [16–18]. To date, many polymers have been successfully electrospun into nanofibers, and electrospun polymer nanofibers with a diameter as small as 5 nm have been reported in the literature. In addition, recent electrospinning technology makes it possible to produce low-cost, high-efficiency ultrathin nanofibers with the variable diameters in the range of nanometers to the micrometers [19–23]. Electrospun nanofiber membranes also have unique features, such as high porosity, good thermal stability and water permeability, interconnected pore structure, and well-controlled compositions. These outstanding features make electrospun

nanofiber membranes an excellent candidate for different applications, such as separation by filtration, self-cleaning textiles, bio-separation, wound healing, and antimicrobial mats. Most importantly, electrospun nanofibers exhibit a large surface-area-to-volume ratio, high porosity, variable pore size, and highly interconnected porous structure, thus making them attractive. In particular, hydrophilic electrospun nanofiber membranes prepared via electrospinning have been extensively researched in fields of film and membrane separation for their ability to remove or reduce micron/submicron-sized particles from solutions.

Cellulose is the most commonly distributed polymer in nature. This is an important biopolymer with exciting features widely available in different natural products, like wood pulp, cotton, hemp, and other plant-based materials [24,25]. Structurally, it is composed of closely associated units with a complex molecular structure, along with polysaccharides and lignin in the plant cell wall [26]. Basically, it is derived from esterification of cellulose, which is obtained via the reaction of cellulose with acetic anhydride and acetic acid in the presence of sulfuric acid. Moreover, CA possesses good fiber-forming capability, promoting new formulations and applications. Cellulose is also present in hemicellulose form in the cell wall, along with lignin and other extractives [27,28]. The nano-sized fibers of cellulose are designed to be microscopic and are often referred to as microfibrils, having diameters in the micrometer range of 2–20 μm, and their lengths depend on their own origin [29–31]. The fibers with uniform and fine structures produced from cellulose show versatile application in different fields, like textile industries, water filtration, pharmaceuticals, food industries, cosmetics, energy storage, and conversion devices [14,15,22,32]. It shows different health-friendly and beneficial properties so that it can be used with other materials as insulators or high-thermal-resistance, cost-effective materials and eco-friendly polymer composite materials [33–36]. Cellulose acetate has several fascinating features, including its biodegradable nature, non-toxicity, high affinity, good hydrolytic stability, relatively low cost, excellent chemical resistance, and non-irritating nature, so it is widely used in the biomedical-related sector and can be used as bioactive molecules after partial chemical modifications [37–40]. In past years, intensive studies have been conducted in regard to understanding the microfiltration of electrospun fibers [41]. Shin and coworkers fabricated nonwoven coalescence filtering media for separating secondary dispersions, using Nylon-6, polyamide, polyacrylonitrile, and polystyrene [42]. For instance, Ma utilized surface functionalized CA mats for successful separation of biomolecules in water [43]. CA membranes have been used for reverse osmosis for the conversion of contaminated water into fresh water and blood dialysis. Chou et al. reported using composites of silver nanoparticles and cellulose acetate hollow fiber membrane for water treatment [44]. The above studies have carried out a series of complex compositions for the fabrication of the nanofibers. CA nanofibers' membranes have an excellent performance for low-molecular-weight toxic contaminants. Also, they have an excellent hydrophilicity, which is a very important factor in the minimization of fouling [45,46]. Moreover, CA membranes exhibit good toughness, high biocompatibility and hydrophilicity, moderate chlorine resistance, good desalting properties, and a high flux capacity [47,48]. Compared to commercially available filtering materials produced via a conventional technique, the pore size distribution of the electrospun nanofibers can effectively be tuned in the range of sub-microns to a few micrometers simply by adjusting the process parameters of the electrospinning [49]. Electrospun CA nanofibers are also capable of maintaining high porosity, which ensures the high-flux liquid filtrations [47,50,51]. However, CA membranes usually suffers from a narrow operating pH range and are susceptible to biological attack and structural compaction at variable temperatures and pressures [52]. Besides, due to poor inter-fiber interaction, which was impacted by physical entanglements, electrospun pure CA nanofibers usually have an unsatisfactory microstructure and poor mechanical strength. Hence, improving the morphology and mechanical properties of CA nanofibers is critical. The incorporation of nanoscale fibers with good mechanical strength into CA nanofibers is an effective method to produce high-performance composite nanofibers. Therefore, it is urgent to maximize the performance of CA membranes by optimizing the porous structures. Moreover, this issues

can be overcome by the selection of polymer solvents, concentrations, additives, solvent evaporation time, and other parameters during membrane processing [53]. Process modifications to increase fiber–fiber interactions and the reinforcing of electrospun fibers using nanoparticles are becoming a highly promising route to address this issue. In addition, biofouling is a significant and constant problem with membrane filtration and specifically for hydrophobic cellulose acetate membranes. Methods to address biofouling can include mechanical or chemical cleaning operations, but another area of focus is the manipulation of the surface chemistry of the membranes to create a surface inhospitable for biofilm formation [29,37]. Miao et al. reported the fabrication of structure-controllable three-dimensional CA nanofibers via adjusting the humidity in the electrospinning process. The cytocompatibilities of 3D nanofibers were found to be better than those of 2D nanofibers and were expected to be used in biodegradable scaffold applications [54]. Lee et al. reported coating of electrospun CA mats with chitin nanocrystals, whose surface had homogenous nanostructured networks, and the mats had tailored surface characteristics [55]. The prepared nanofibers exhibited high water flux and less fouling; thus, they could be applied to water purification in the food industry. Mahalingam et al. devised a new route to synthesize CA/PAN composite fiber by pressurized gyration [56]. Consequently, well-characterized self-generating porous composite fibers were obtained by carefully tuning the parameters of the working pressure. Bui et al. fabricated a hydrophilic PAN/CA fiber in DMF at different weight ratios for engineered osmosis via a combination of nanotechnology and membrane science. The results showed that the CA/PAN composite fiber possessed excellent perm selectivity. These composite fibers have potential applications for engineered osmosis [57]. Silva et al. prepared CA membranes using nanoparticles as additives [58]. These composite nanofibers exhibited enhanced physicochemical properties and good performance as adsorbents, as well as anti-biofouling agents. Similarly, a quaternary ammonium-propylated polysilsesquioxane (QPAS)/cellulose acetate membrane prepared by Ravi et al. demonstrated excellent water permeability [59]. Meanwhile, Ansari et al. prepared an amphiphilic cellulose membrane incorporated with molybdenum disulfide for oil–water separation [60]. The resultant membrane showed a high water flux under different conditions, such as initial oil concentration, salt concentration, and pH conditions, and such results might be attributed to the hydrophilic support of the cellulose acetate polymer. Several research studies based on ion mixed-matrix nanoporous membranes have been reported by incorporating organic/inorganic compounds [61,62]. However, a functionally graded membrane (FGM) with a special spiral-structured cellulose acetate (CA) membrane prepared by a single-step electrospinning process is yet to be discovered.

A number of processing parameters influence the electrospinning of polymer solutions, which ultimately determine and control the properties of the fabricated nano-fibrous membrane. The concentration of polymer, solvent type, flow rate, distance between nozzle tip and collector, and applied voltage affects the morphology of nano-membrane. Similarly, the physical and environmental parameters, like the operating temperature and humidity, are also responsible for controlling the nature of fiber [19]. The schematic representation of the electrospinning technique for the fabrication of the cellulose acetate membrane is outlined in Figure 1. It focuses on the impact of different cellulose concentrations, as well as different collection distances on the fiber morphology. The low concentration of CA showed the presence of beads and tiny fibers. Upon increasing the concentration homogeneous, smooth fibers were formed, which were also favorable for excellent water permeation flux. Here, two different approaches of electrospinning were carried out: first by nano-membrane collection on the same plate under different distances and second by collection on the same plate by automatically moving the collector drum between the fixed distances of the spinneret tip to collector drum. By this method, the functionally graded membrane having a special spiral structure on CA membrane was successfully designed. This showed that the as-fabricated CA membrane is much better for water filtration with a high water permeation flux, making it beneficial for the transport of aqueous media from one place to other. Loading some extra functional nanoparticles on different layers of the

functionally graded membrane of the special spiral structure will add more benefits for diverse use in tissue engineering or biomedical fields.
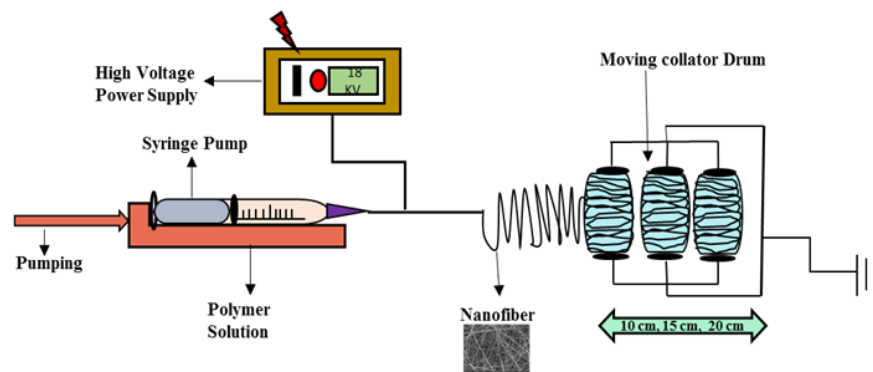

Figure 1. Schematic diagram showing fabrication process of functionally graded CA membrane by auto-controlled electrospinning process.

2. Materials and Methods

2.1. Materials

Cellulose acetate (CA, MW = 50,000) was purchased from Daejung Chemicals & Metals Co. Ltd., Daejeon, Republic of Korea. Acetone, N, N-Dimethylacetamide (99.5%) (DMAc), and sodium hydroxide (NaOH) were purchased from Samchun Chemicals Co. Ltd., Seoul, Republic of Korea. All the chemicals were of research grade and used without purification. Deionized water was used throughout this work. Electrospinning was carried out using a NanoNC electrospinning system.

2.2. Fabrication of Nano-Membrane

Cellulose acetate (CA) of 15 wt.% was dissolved in the solvent mixture of acetone and DMAc at a weight ratio of 2:1. The CA mixture was stirred on the magnetic stirrer at 250 rpm for 6 h, under a stirring temperature of 60 °C. The CA solution was loaded on a 12 mL plastic syringe (Norm-Ject, Duisburg, Germany) and connected with a metal capillary tube (d = 0.51 mm, 21 G) via a plastic tube. The solution was pumped by a digital pump (New Era Pump System, Inc., Farmingdale, NY, USA), with a constant flow rate of 1 mL/h. The distance between the collector drum and spinneret tip varied—10, 15, and 20 cm—with an applied voltage of 15 kV. During fabrication, the fiber was collected on the polyethylene sheet wrapped around the rotating aluminum mandrel connected with a negative pole of applied voltage, while the spinneret connected with a positive pole. The auto-controlled electrospinning was carried out at 27 °C (room temperature), with the relative humidity at 45–55%. During the process, the nozzle moved horizontally on its axial distance of 10 to 145 mm with the linear speed of 100 mm/min. With these set up, the total membrane collection time was 6 h.

2.3. Post-Electrospinning Treatment

The electrospun cellulose acetate (CA) membrane was deacetylated into hydrophilic cellulose via alkaline hydrolysis with 0.05 M NaOH solution. The aqueous ethanolic solution was prepared by dissolving the calculated amount of NaOH in water and then with ethanol to make the volume-by-volume solvent ratio of 1:4. The CA membrane was immersed in NaOH solution for 24 h to generate hydrophilic CA. After the completion of hydrolysis, the membrane was washed copiously with DI-water to remove any residual reactants and dried under vacuum for 12 h at 60 °C.

2.4. Characterization

The morphology of membrane was examined by field emission scanning electron microscopy (FESEM, S-7400, 200 kV, Hitachi, Tokyo, Japan). The SEM images of membrane

were further analyzed by ImageJ (Version 2) software to obtain the fiber diameter. The crystallographic structure was investigated by powder X-ray diffraction (XRD, Rigaku, Cu Kα λ = 1.540 Ao, 30 kV, 40 mA). The water flux permeability test was carried out using 50 mL Amicon stirred cells (UFSC05001, Billerica, MA, USA).

2.5. Water Permeability Test

The water permeability test of the as-fabricated membrane was carried out using Amicon stirred cells, and it was able to operate at a maximum working pressure of 75 psi, with a 50 mL feeding capacity. Nitrogen gas was used for external pressure on the feed water, and the water permeability of the membrane was compared by measuring the time required to pass the equal volume of pure water through the as-fabricated membranes under similar conditions. Four different pressures as 0, 5, 10, and 15 psi were used for the measurement of water flux. Here, 50 mL of pure DI-water was allowed to pass through the fibrous membrane of 44.5 mm in diameter, with an effective area of 13.4 cm^2 in Amicon stirred cells at room temperature.

3. Results and Discussion

3.1. Morphology

3.1.1. Effect of Concentration

The morphology of the electrospun fibrous membrane is greatly affected by the concentration of polymer solution. At a low concentration, large numbers of bead structures were formed. Figure 2a shows the FESEM image of 8 wt.% CA fiber collected at a 15 cm distance between the spinneret tip and collector drum. Here, CA undergoes electrospray due to the jet breaking up into the droplets, resulting in the formation of spherical beads rather than fibers. During this, when the solvent is evaporated from the beads, a vacant space is formed inside, which undergoes structural collapse into a cavity due to the atmospheric pressure [20]. If the solvent did not evaporate completely, then the beads may coagulate with each other to form the big solid lumps. Solid beads are generally obtained at a comparatively low solvent evaporation rate within the small collection distance. Upon the gradual increase in concentration, the spherical beads start to change into spindle and elongated-spindle shapes. The concentration shows a change in the aspect ratio of the nanofibers. The aspect ratio of the nanofibers increases continuously with the increasing concentration of the polymer. Figure 2b shows the special bird's nest-like elongated-spindle shape beaded fiber collected from 13 wt.% at 15 cm. CA of 15 wt.% showed the formation of smooth, homogenous fibrous membranes with a comparatively small diameter distribution range (as shown in Figure 3b). The fully wetted and interconnected porous network will yield a support material that will create a membrane with one of the lowest possible structural parameters to date and maximize osmotic water flux performance. At an excessively high concentration, the thick polymer solution blocks off the nozzle tip, making it difficult to perform electrospinning. The high concentration shows the formation of fibers with irregular diameters and a large diameter distribution range. The crystallographic properties and chemical compositions of the samples were evaluated by XRD. Figure 2c shows the XRD patterns of CA fiber. A broad peak at 2θ 21–23° indicates the cellulose acetate [63]. The CA membrane was deacetylated into hydrophilic cellulose by alkaline hydrolysis with 0.05 M NaOH solution. An FTIR analysis was performed to study the change in the chemical structure of CA nanofibers after NaOH treatment for deacetylation (Figure 2d). As can be seen in Figure 2d, the CA nanofibers showed characteristic peaks of cellulose acetate at 1741.9 cm^{-1}, 1365.6 cm^{-1}, and 1227.61 cm^{-1}, which is attributed to the C=O, C-CH$_3$, and C-O-C vibrations. The characteristic peaks of CA disappeared after deacetylation, implying the elimination of acetate groups. On the contrary, the peak intensity of the -OH group increases significantly.
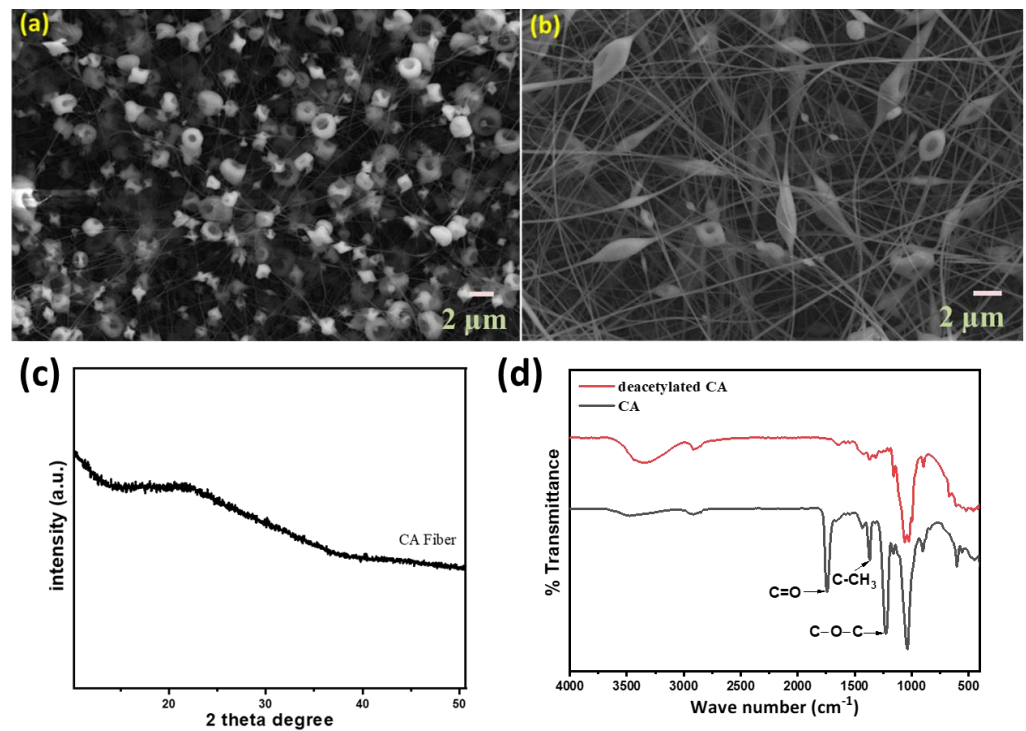
Figure 2. FESEM images of (**a**) 8 wt.% CA fiber, (**b**) 13 wt.% CA fiber, (**c**) XRD pattern of 13 wt.% CA fiber, and (**d**) FTIR spectra of CA and deacetylated CA nanofibers.
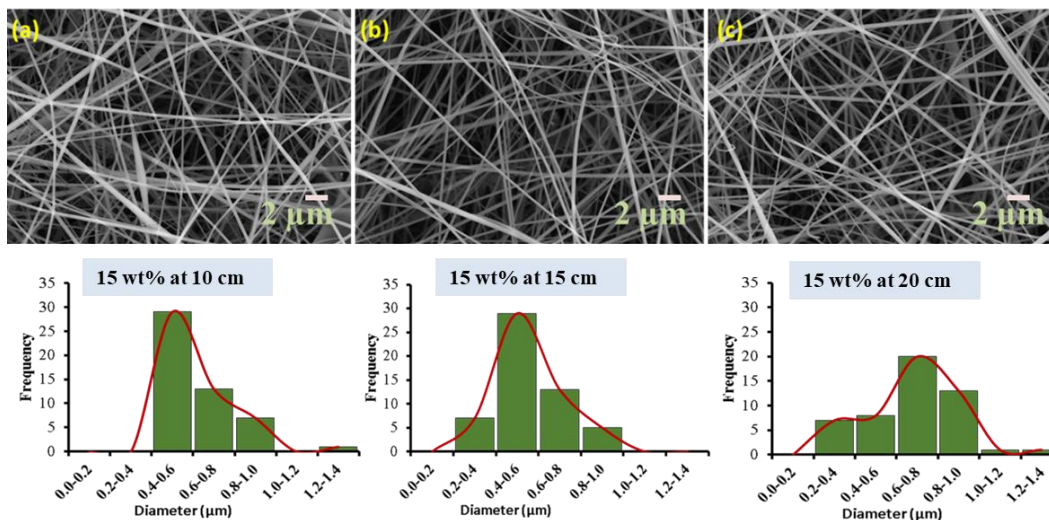

Figure 3. FESEM images of 15 wt.% CA membrane collected at (**a**) 10 cm, (**b**) 15 cm, and (**c**) 20 cm. Fiber diameter given below with corresponding images.

3.1.2. Effect of Distance

The distance between the nozzle tip and the collector of fiber shows the pronounced effect on the fiber deposition time, solvent evaporation rate, strength of applied voltage, and polymer jet instability time interval [64]. The applied electric field becomes very strong at very short distances, thus enhancing the instability of the jet solution, resulting in the multiple jets of the polymer coming out from the single nozzle tip. CA of 15 wt.% was used for the electrospinning at different collection distances. The different distances between the nozzle tip and collector drum experience different electrostatic forces of attraction, bringing versatility to the fiber diameter. The fiber collected at a short distance of 10 cm experiences the strong electrostatic force, resulting in the short flight time for the polymer jet. This causes the bending instability of polymer jet forming the comparatively thick

fiber diameters, as shown in Figure 3a. The fiber collected at 15 cm shows the presence of a smooth, homogeneous diameter (Figure 3b). These fibers show a small diameter distribution range. This indicates that the polymer jet sprayed at this distance experiences the optimum and stable electrostatic pull, which results in the formation of homogeneous fibers. At a higher distance of 20 cm, the polymer jet experiences a weak electrostatic force of attraction, and, because of this, it gains high floating time in air. This leads to the formation of thin fibers (Figure 3c).

From this, it is concluded that the homogeneous fiber can be collected from 15 wt.% CA at the distance of 15 cm. This smooth, homogeneous fiber with a special morphological structure will be more beneficial for diverse application. The collection of fibers at different distances from the spinneret tip to the collector drum suggested the clear distinction of fiber diameters, making them useful for fabricating the fibrous membrane of the special structure. The fiber was collected on the same plate at different distances (10, 15, and 20 cm) between the spinneret and collector drum, with a fixed collection time of 2 h at each distance to obtain the special spiral structure. Here, the total fiber collection time was 6 h at three different distances. Figure 4a shows the surface FESEM of the fibrous membrane of 15 wt.% CA collected at different distances on the same plate, and Figure 4b shows the cross-section of it, showing the three distinct fiber layers with clear variations in diameters, as doing so is important to outline the functionally graded membrane (FGM)'s special spiral structure. The collection of the fibrous membrane at 10, 15, and 20 cm formed the upper layer with fine fibers with small diameters, and the diameter increases moving onward. This leads to the formation of a finer and bigger pore size in the upper layer; meanwhile, the small pore size in the inner fiber layer collected at 10 cm is due to the presence of thick fibers [65]. The presence of a hollow spiral channel in the fibrous membrane collected at three different distances on the same plate is very useful for the transfer of liquids from one end to the other end.
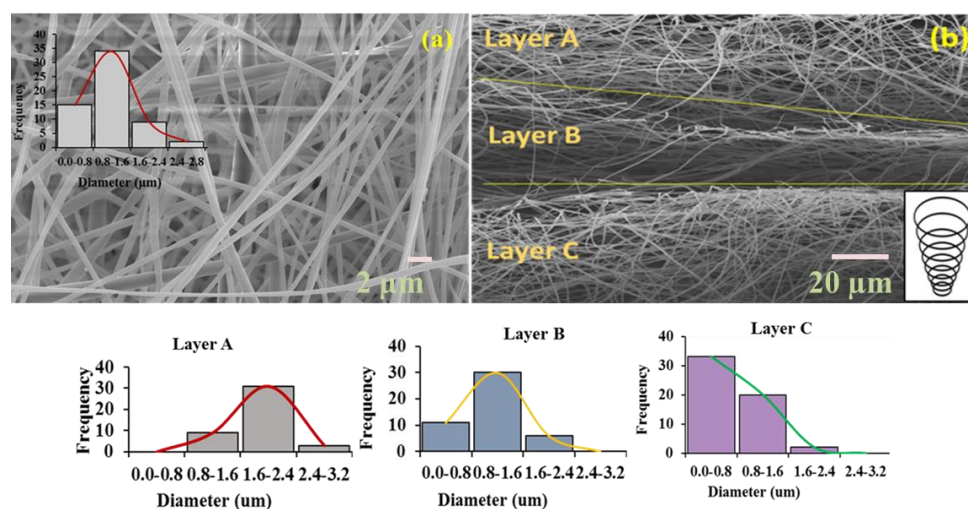

Figure 4. (**a**) FESEM image of fibrous membrane collected at 10, 15, and 20 cm on the same plate for a total of 6 h; and (**b**) its cross-section, along with fiber diameters (inset schematic diagram of spiral structure).

The morphological verification of the spiral structure can also be made by comparing it with a membrane prepared from the opposite collection approach. Figure 5a shows the membrane collected with the distance pattern of 20, 15, and 10 cm on the same plate for a total of 6 h of collection time. The fiber diameter on the membrane surface shows the presence of thick fiber in the 0.8–1.6 μ range because of the upper layer collected at 10 cm. The cross-section image shown in Figure 5b does not show any distinct layers as Figure 4b does, but the average diameter pattern of the fiber is almost the same. This helps to conclude that the membrane is fabricated in the same manner as above to facilitate the formation of a functional graded membrane with a special spiral structure.
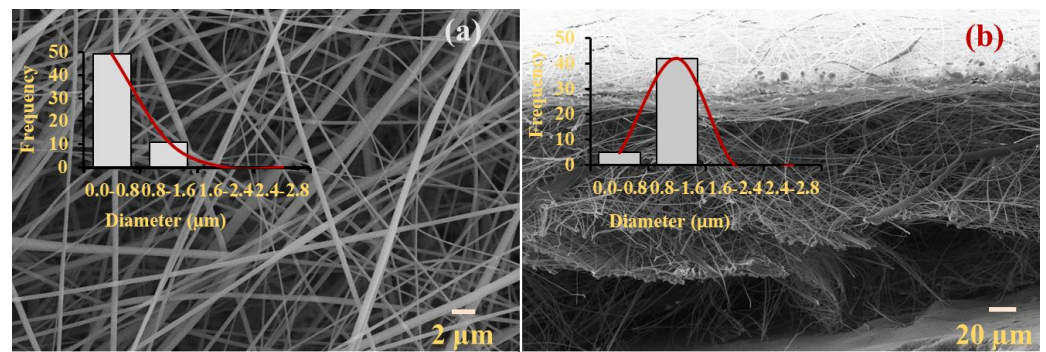
Figure 5. (**a**) FESEM image of CA membrane collected at 20, 15, and 10 cm on same plate for a total of 6 h; (**b**) its cross-section image with their diameter.

The CA membrane was collected using another approach, which involved automatically moving the rotating collector drum between the distances of 10 and 20 cm. The fibrous membrane collected by this approach shows the higher diameter distribution range (Figure 6a). Here, fiber diameters less than 0.8 µ are also observed in a considerable number. A majority of diameters lie in the range of 0.8–1.6 µ, which is same average diameter range of the membranes collected previously by another approach. The collector drum was constantly moving from a minimum of 10 to a maximum of 20 cm, giving the highest diameter range with thick fibers of 2.8 µ. The cross-section image, Figure 6b, shows the harmoniously laying fibers within the large diameter distribution range. This large diameter distribution range also supports the formation of functionally graded membrane with a special spiral structure.
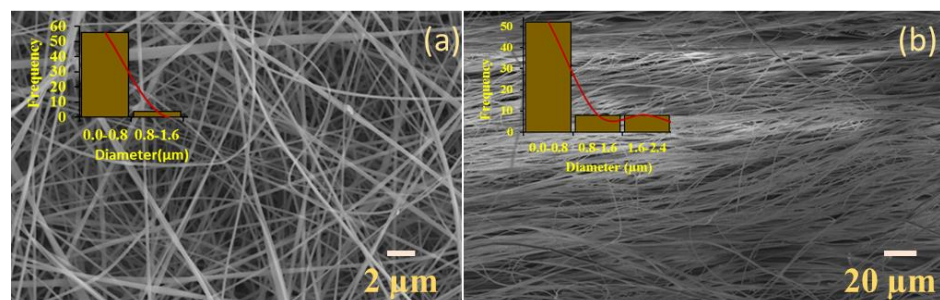

Figure 6. (**a**) FESEM image of fibrous membrane collected by moving drum between the distances of 10 and 20 cm for 6 h; (**b**) its cross-section.

3.2. Water Permeation Flux

Water permeation flux is important to any fibrous membrane designed for practical application for water transport or water purification via a filtration technique. The water flux of different membrane samples was measured under different pressures. Nitrogen gas was used to impart external pressure on the feed water. The water permeation flux of 15 wt.% CA membrane collected at different distances is presented in Figure 7. The smooth, homogenous membrane collected at 15 cm showed better water flux in comparison to the fibrous membrane collected at other distances.

The water permeation flux of the functionally graded membrane with special spiral structure prepared by two different approaches was also tested [66]. The membrane collected at three different distances on the same collecting plate by automatically moving the collector drum between the distances of 10 and 20 cm showed the excellent permeation flux at 15 psi compared to that of the membranes collected at different distances on the same plate and other fibrous membranes collected on different collecting plates at different distances (Figure 8). The high water flux of this membrane may be due to the presence of the functionally graded membrane with a special spiral structure due to the difference in average fiber diameters. This special spiral structure on the CA membrane with high

water permeation flux may be of excellent application for the purpose of water or liquid transport from one face to another.
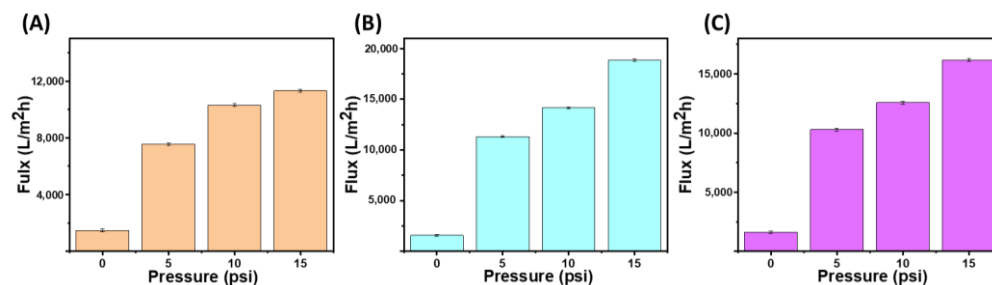

Figure 7. Water flux under different pressures for 15 wt.% CA membrane collected at (**A**) 10 cm, (**B**) 15 cm, and (**C**) 20 cm.
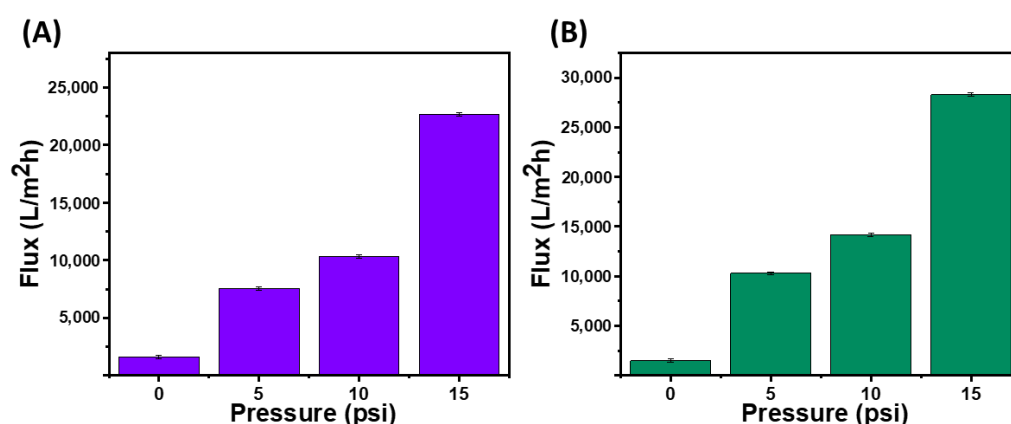

Figure 8. Water permeation flux under different pressures for 15 wt.% CA membrane collected (**A**) on same plate at 10, 15, and 20 cm; and (**B**) by moving collector between 10 and 20 cm.

4. Conclusions

The present study mainly focuses on the effect of the concentration of cellulose acetate and the different fiber collection distances during the auto-controlled electrospinning process for the fabrication of a functionally graded membrane with a special spiral structure. The change in fiber diameter depends on the concentration of cellulose acetate and also on the fiber collection distances. At a high concentration, the more viscous polymer solution results in the formation of a thick fiber. Upon increasing the collection distance, the polymer jet gets enough time to fly in air before reaching the collector drum with enough elongation, resulting in the thin fiber. The diameter was directly affected by the fiber collection distance. This principle is applied for the fabrication of a functionally graded membrane with a special spiral structure on the fibrous membrane. The continuous one-step automatic electrospinning of cellulose acetate at three different distances on the same collecting plate was carried out to design a functionally graded membrane with a special spiral structure. This special structure of the fibrous membrane is of great importance for application in the liquid transport from one destination to another, which is very useful for tissue engineering, drug delivery, water filtration, etc. The functionally graded membrane with a special spiral structure prepared by two different approaches demonstrates high water permeation flux.

Data Availability Statement: The original contributions presented in the study are included in the article, further inquiries can be directed to the corresponding authors.

Conflicts of Interest: All co-authors have contributed to this work and are aware of this submission. The authors do not have conflict of interest for submitting this manuscript in this journal.

References

1. Ramakrishna, S.; Fujihara, K.; Teo, W.-E.; Yong, T.; Ma, Z.; Ramaseshan, R. Electrospun nanofibers: Solving global issues. *Mater. Today* **2006**, *9*, 40–50. [CrossRef]
2. Kausar, A.; Ahmad, I. Electrospinning Processing of Polymer/Nanocarbon Nanocomposite Nanofibers—Design, Features, and Technical Compliances. *J. Compos. Sci.* **2023**, *7*, 290. [CrossRef]
3. Zeleny, J. The electrical discharge from liquid points, and a hydrostatic method of measuring the electric intensity at their surfaces. *Phys. Rev.* **1914**, *3*, 69. [CrossRef]
4. Formhals, A. Process and Apparatus for Preparing Artificial Threads. U.S. Patent No. 1,975,504, 2 January 1934.
5. Torres-Giner, S.; Gimenez, E.; Lagarón, J.M. Characterization of the morphology and thermal properties of zein prolamine nanostructures obtained by electrospinning. *Food Hydrocoll.* **2008**, *22*, 601–614. [CrossRef]
6. Reneker, D.H.; Yarin, A.L. Electrospinning jets and polymer nanofibers. *Polymer* **2008**, *49*, 2387–2425. [CrossRef]
7. Bognitzki, M.; Czado, W.; Frese, T.; Schaper, A.; Hellwig, M.; Steinhart, M.; Greiner, A.; Wendorff, J.H. Nanostructured fibers via electrospinning. *Adv. Mater.* **2001**, *13*, 70–72. [CrossRef]
8. Li, D.; Xia, Y. Electrospinning of Nanofibers: Reinventing the Wheel? *Adv. Mater.* **2004**, *16*, 1151–1170. [CrossRef]
9. Liao, Y.; Loh, C.-H.; Tian, M.; Wang, R.; Fane, A.G. Progress in electrospun polymeric nanofibrous membranes for water treatment: Fabrication, modification and applications. *Prog. Polym. Sci.* **2018**, *77*, 69–94. [CrossRef]
10. Sun, B.; Long, Y.Z.; Zhang, H.D.; Li, M.M.; Duvail, J.L.; Jiang, X.Y.; Yin, H.L. Advances in three-dimensional nanofibrous macrostructures via electrospinning. *Prog. Polym. Sci.* **2014**, *39*, 862–890. [CrossRef]
11. Tan, S.; Inai, R.; Kotaki, M.; Ramakrishna, S. Systematic parameter study for ultra-fine fiber fabrication via electrospinning process. *Polymer* **2005**, *46*, 6128–6134. [CrossRef]
12. Xue, J.; Wu, T.; Dai, Y.; Xia, Y. Electrospinning and Electrospun Nanofibers: Methods, Materials, and Applications. *Chem. Rev.* **2019**, *119*, 5298–5415. [CrossRef] [PubMed]
13. He, X.-X.; Zheng, J.; Yu, G.-F.; You, M.-H.; Yu, M.; Ning, X.; Long, Y.-Z. Near-field electrospinning: Progress and applications. *J. Phys. Chem. C* **2017**, *121*, 8663–8678. [CrossRef]
14. Poudel, M.B.; Awasthi, G.P.; Kim, H.J. Novel insight into the adsorption of Cr(VI) and Pb(II) ions by MOF derived Co-Al layered double hydroxide @hematite nanorods on 3D porous carbon nanofiber network. *Chem. Eng. J.* **2021**, *417*, 129312. [CrossRef]
15. Poudel, M.B.; Kim, H.J. Confinement of Zn-Mg-Al-layered double hydroxide and α-Fe$_2$O$_3$ nanorods on hollow porous carbon nanofibers: A free-standing electrode for solid-state symmetric supercapacitors. *Chem. Eng. J.* **2022**, *429*, 132345. [CrossRef]
16. Cheryan, M.; Rajagopalan, N. Membrane processing of oily streams. Wastewater treatment and waste reduction. *J. Membr. Sci.* **1998**, *151*, 13–28. [CrossRef]
17. Viswanathamurthi, P.; Bhattarai, N.; Kim, C.K.; Kim, H.Y.; Lee, D.R. Ruthenium doped TiO$_2$ fibers by electrospinning. *Inorg. Chem. Commun.* **2004**, *7*, 679–682. [CrossRef]
18. Mobaraki, M.; Liu, M.; Masoud, A.-R.; Mills, D.K. Biomedical Applications of Blow-Spun Coatings, Mats, and Scaffolds—A Mini-Review. *J. Compos. Sci.* **2023**, *7*, 86. [CrossRef]
19. Huang, Z.-M.; Zhang, Y.Z.; Kotaki, M.; Ramakrishna, S. A review on polymer nanofibers by electrospinning and their applications in nanocomposites. *Compos. Sci. Technol.* **2003**, *63*, 2223–2253. [CrossRef]
20. Vonnegut, B.; Neubauer, R.L. Production of monodisperse liquid particles by electrical atomization. *J. Colloid Sci.* **1952**, *7*, 616–622. [CrossRef]
21. Thavasi, V.; Singh, G.; Ramakrishna, S. Electrospun nanofibers in energy and environmental applications. *Energy Environ. Sci.* **2008**, *1*, 205–221. [CrossRef]
22. Babu Poudel, M.; Shin, M.; Joo Kim, H. Interface engineering of MIL-88 derived MnFe-LDH and MnFe$_2$O$_3$ on three-dimensional carbon nanofibers for the efficient adsorption of Cr(VI), Pb(II), and As(III) ions. *Sep. Purif. Technol.* **2022**, *287*, 120463. [CrossRef]
23. Lohani, P.C.; Tiwari, A.P.; Muthurasu, A.; Pathak, I.; Poudel, M.B.; Chhetri, K.; Dahal, B.; Acharya, D.; Ko, T.H.; Kim, H.Y. Phytic acid empowered two nanos "Polypyrrole tunnels and transition Metal-(Oxy)hydroxide Sheets" in a single platform for unmitigated redox water splitting. *Chem. Eng. J.* **2023**, *463*. [CrossRef]
24. Raven, J.A. The evolution of vascular land plants in relation to supracellular transport processes. In *Advances in Botanical Research*; Elsevier: Amsterdam, The Netherlands, 1977; Volume 5, pp. 153–219.
25. Zhang, Y.; Zhang, C.; Wang, Y. Recent progress in cellulose-based electrospun nanofibers as multifunctional materials. *Nanoscale Adv.* **2021**, *3*, 6040–6047. [CrossRef]
26. Alemdar, A.; Sain, M. Isolation and characterization of nanofibers from agricultural residues—Wheat straw and soy hulls. *Bioresour. Technol.* **2008**, *99*, 1664–1671. [CrossRef] [PubMed]
27. Lu, Y.; He, Q.; Fan, G.; Cheng, Q.; Song, G. Extraction and modification of hemicellulose from lignocellulosic biomass: A review. *Green Process. Synth.* **2021**, *10*, 779–804. [CrossRef]

28. Barhoum, A.; Jeevanandam, J.; Rastogi, A.; Samyn, P.; Boluk, Y.; Dufresne, A.; Danquah, M.K.; Bechelany, M. Plant celluloses, hemicelluloses, lignins, and volatile oils for the synthesis of nanoparticles and nanostructured materials. *Nanoscale* **2020**, *12*, 22845–22890. [CrossRef]

29. Rijal, M.S.; Nasir, M.; Purwasasmita, B.S.; Asri, L.A.T.W. Cellulose nanocrystals-microfibrils biocomposite with improved membrane performance. *Carbohydr. Polym. Technol. Appl.* **2023**, *5*, 100326. [CrossRef]

30. Li, K.; McGrady, D.; Zhao, X.; Ker, D.; Tekinalp, H.; He, X.; Qu, J.; Aytug, T.; Cakmak, E.; Phipps, J.; et al. Surface-modified and oven-dried microfibrillated cellulose reinforced biocomposites: Cellulose network enabled high performance. *Carbohydr. Polym.* **2021**, *256*, 117525. [CrossRef]

31. Khalili, H.; Bahloul, A.; Ablouh, E.-H.; Sehaqui, H.; Kassab, Z.; Semlali Aouragh Hassani, F.-Z.; El Achaby, M. Starch biocomposites based on cellulose microfibers and nanocrystals extracted from alfa fibers (*Stipa tenacissima*). *Int. J. Biol. Macromol.* **2023**, *226*, 345–356. [CrossRef]

32. Tournilhac, F.; Lorant, R. Composition in the Form of an Oil-in-Water Emulsion Containing Cellulose Fibrils, and Its Uses, Especially Cosmetic Uses. U.S. Patent 6,534,071, 18 March 2003.

33. Hong, F.; Zhu, Y.X.; Yang, G.; Yang, X.X. Wheat straw acid hydrolysate as a potential cost-effective feedstock for production of bacterial cellulose. *J. Chem. Technol. Biotechnol.* **2011**, *86*, 675–680. [CrossRef]

34. Prevost, T.; Oommen, T. Cellulose insulation in oil-filled power transformers: Part I-history and development. *IEEE Electr. Insul. Mag.* **2006**, *1*, 28–35. [CrossRef]

35. Sobsey, M.D.; Stauber, C.E.; Casanova, L.M.; Brown, J.M.; Elliott, M.A. Point of use household drinking water filtration: A practical, effective solution for providing sustained access to safe drinking water in the developing world. *Environ. Sci. Technol.* **2008**, *42*, 4261–4267. [CrossRef]

36. Park, H.-M.; Misra, M.; Drzal, L.T.; Mohanty, A.K. "Green" nanocomposites from cellulose acetate bioplastic and clay: Effect of eco-friendly triethyl citrate plasticizer. *Biomacromolecules* **2004**, *5*, 2281–2288. [CrossRef]

37. Wan, Y.; Huang, Y.; Yuan, C.; Raman, S.; Zhu, Y.; Jiang, H.; He, F.; Gao, C. Biomimetic synthesis of hydroxyapatite/bacterial cellulose nanocomposites for biomedical applications. *Mater. Sci. Eng. C* **2007**, *27*, 855–864. [CrossRef]

38. Dharmaraj, N.; Park, H.C.; Lee, B.M.; Viswanathamurthi, P.; Kim, H.Y.; Lee, D.R. Preparation and morphology of magnesium titanate nanofibres via electrospinning. *Inorg. Chem. Commun.* **2004**, *7*, 431–433. [CrossRef]

39. Cellante, L.; Costa, R.; Monaco, I.; Cenacchi, G.; Locatelli, E. One-step esterification of nanocellulose in a Brønsted acid ionic liquid for delivery to glioblastoma cancer cells. *New J. Chem.* **2018**, *42*, 5237–5242. [CrossRef]

40. Tortorella, S.; Maturi, M.; Dapporto, F.; Spanu, C.; Sambri, L.; Comes Franchini, M.; Chiariello, M.; Locatelli, E. Surface modification of nanocellulose through carbamate link for a selective release of chemotherapeutics. *Cellulose* **2020**, *27*, 8503–8511. [CrossRef]

41. Han, J.-C.; Xing, X.-Y.; Wang, J.; Wu, Q.-Y. Preparation and Properties of Thin-Film Composite Forward Osmosis Membranes Supported by Cellulose Triacetate Porous Substrate via a Nonsolvent-Thermally Induced Phase Separation Process. *Membranes* **2022**, *12*, 412. [CrossRef] [PubMed]

42. Shin, C.; Chase, G.G. Water-in-oil coalescence in micro-nanofiber composite filters. *AIChE J.* **2004**, *50*, 343–350. [CrossRef]

43. Ma, Z.; Kotaki, M.; Ramakrishna, S. Electrospun cellulose nanofiber as affinity membrane. *J. Membr. Sci.* **2005**, *265*, 115–123. [CrossRef]

44. Chou, W.-L.; Yu, D.-G.; Yang, M.-C. The preparation and characterization of silver-loading cellulose acetate hollow fiber membrane for water treatment. *Polym. Adv. Technol.* **2005**, *16*, 600–607. [CrossRef]

45. Abedini, R.; Mousavi, S.M.; Aminzadeh, R. A novel cellulose acetate (CA) membrane using TiO2 nanoparticles: Preparation, characterization and permeation study. *Desalination* **2011**, *277*, 40–45. [CrossRef]

46. Yu, X.; Zhang, X.; Xing, Y.; Zhang, H.; Jiang, W.; Zhou, K.; Li, Y. Development of Janus Cellulose Acetate Fiber (CA) Membranes for Highly Efficient Oil–Water Separation. *Materials* **2021**, *14*, 5916. [CrossRef] [PubMed]

47. Silva, M.A.; Belmonte-Reche, E.; de Amorim, M.T.P. Morphology and water flux of produced cellulose acetate membranes reinforced by the design of experiments (DOE). *Carbohydr. Polym.* **2021**, *254*, 117407. [CrossRef] [PubMed]

48. Yin, C.; Wang, S.; Zhang, Y.; Chen, Z.; Lin, Z.; Fu, P.; Yao, L. Correlation between the pore resistance and water flux of the cellulose acetate membrane. *Environ. Sci. Water Res. Technol.* **2017**, *3*, 1037–1041. [CrossRef]

49. El Badawi, N.; Ramadan, A.R.; Esawi, A.M.K.; El-Morsi, M. Novel carbon nanotube–cellulose acetate nanocomposite membranes for water filtration applications. *Desalination* **2014**, *344*, 79–85. [CrossRef]

50. Sabir, A.; Shafiq, M.; Islam, A.; Jabeen, F.; Shafeeq, A.; Ahmad, A.; Zahid Butt, M.T.; Jacob, K.I.; Jamil, T. Conjugation of silica nanoparticles with cellulose acetate/polyethylene glycol 300 membrane for reverse osmosis using MgSO$_4$ solution. *Carbohydr. Polym.* **2016**, *136*, 551–559. [CrossRef] [PubMed]

51. Gantzel, P.K.; Merten, U. Gas Separations with High-Flux Cellulose Acetate Membranes. *Ind. Eng. Chem. Process Des. Dev.* **1970**, *9*, 331–332. [CrossRef]

52. Park, H.B.; Freeman, B.D.; Zhang, Z.-B.; Sankir, M.; McGrath, J.E. Highly Chlorine-Tolerant Polymers for Desalination. *Angew. Chem. Int. Ed.* **2008**, *47*, 6019–6024. [CrossRef]

53. Han, B.; Zhang, D.; Shao, Z.; Kong, L.; Lv, S. Preparation and characterization of cellulose acetate/carboxymethyl cellulose acetate blend ultrafiltration membranes. *Desalination* **2013**, *311*, 80–89. [CrossRef]

54. Cheng, M.; Qin, Z.; Hu, S.; Yu, H.; Zhu, M. Use of electrospinning to directly fabricate three-dimensional nanofiber stacks of cellulose acetate under high relative humidity condition. *Cellulose* **2017**, *24*, 219–229. [CrossRef]

55. Goetz, L.A.; Jalvo, B.; Rosal, R.; Mathew, A.P. Superhydrophilic anti-fouling electrospun cellulose acetate membranes coated with chitin nanocrystals for water filtration. *J. Membr. Sci.* **2016**, *510*, 238–248. [CrossRef]

56. Mahalingam, S.; Wu, X.; Edirisinghe, M. Evolution of self-generating porous microstructures in polyacrylonitrile-cellulose acetate blend fibres. *Mater. Des.* **2017**, *134*, 259–271. [CrossRef]

57. Bui, N.-N.; McCutcheon, J.R. Hydrophilic Nanofibers as New Supports for Thin Film Composite Membranes for Engineered Osmosis. *Environ. Sci. Technol.* **2013**, *47*, 1761–1769. [CrossRef] [PubMed]

58. Silva, M.A.; Hilliou, L.; de Amorim, M.T.P. Fabrication of pristine-multiwalled carbon nanotubes/cellulose acetate composites for removal of methylene blue. *Polym. Bull.* **2020**, *77*, 623–653. [CrossRef]

59. Pandey, R.P.; Kallem, P.; Rasheed, P.A.; Mahmoud, K.A.; Banat, F.; Lau, W.J.; Hasan, S.W. Enhanced water flux and bacterial resistance in cellulose acetate membranes with quaternary ammoniumpropylated polysilsesquioxane. *Chemosphere* **2022**, *289*, 133144. [CrossRef] [PubMed]

60. Al Ansari, Z.; Arshad, F.; Nghiem, L.D.; Zou, L. Amphiphilic cellulose acetate membrane incorporated with MoS2 nanospheres for oil in water separation. *Environ. Sci. Water Res. Technol.* **2022**, *8*, 2694–2704. [CrossRef]

61. Thangavelu, K.; Zou, L. Evaluating oil removal by amphiphilic MoS2/cellulose acetate fibrous sponge in a flow-through reactor and by artificial neural network. *Environ. Nanotechnol. Monit. Manag.* **2022**, *18*, 100684. [CrossRef]

62. Azam, R.S.; Almasri, D.A.; Alfahel, R.; Hawari, A.H.; Hassan, M.K.; Elzatahry, A.A.; Mahmoud, K.A. MXene (Ti$_3$C$_2$Tx)/Cellulose Acetate Mixed-Matrix Membrane Enhances Fouling Resistance and Rejection in the Crossflow Filtration Process. *Membranes* **2022**, *12*, 406. [CrossRef]

63. Prakash, J.; Venkataprasanna, K.S.; Bharath, G.; Banat, F.; Niranjan, R.; Venkatasubbu, G.D. In-vitro evaluation of electrospun cellulose acetate nanofiber containing Graphene oxide/TiO$_2$/Curcumin for wound healing application. *Colloids Surf. A Physicochem. Eng. Asp.* **2021**, *627*, 127166. [CrossRef]

64. Subbiah, T.; Bhat, G.; Tock, R.; Parameswaran, S.; Ramkumar, S. Electrospinning of nanofibers. *J. Appl. Polym. Sci.* **2005**, *96*, 557–569. [CrossRef]

65. Podgórski, A.; Bałazy, A.; Gradoń, L. Application of nanofibers to improve the filtration efficiency of the most penetrating aerosol particles in fibrous filters. *Chem. Eng. Sci.* **2006**, *61*, 6804–6815. [CrossRef]

66. Kausar, A.; Bocchetta, P. Polymer/Graphene Nanocomposite Membranes: Status and Emerging Prospects. *J. Compos. Sci.* **2022**, *6*, 76. [CrossRef]